Turkish Journal of Electrical Engineering & Computer Sciences

http://journals.tubitak.gov.tr/elektrik/

Research Article

Turk J Elec Eng & Comp Sci
(2017) 25: 3713 – 3724

doi:10.3906/elk-1606-144

Space-time block coded spatial modulation scheme enhanced by employing an intersymbol phase and power allocation

Ahmet Faruk COŞKUN*
Informatics and Information Security Research Center, Scientific and Technological Research Council of Turkey, Kocaeli, Turkey

Received: 10.06.2016 • **Accepted/Published Online:** 13.03.2017 • **Final Version:** 05.10.2017

Abstract: This paper provides a brief and insightful examination of the advantages achieved by employing combined phase offsetting and power allocation mechanisms in the space-time block coded (STBC) transmission of spatial modulation schemes with cyclic structure (CSM). In order to achieve increased coding gain distances (CGDs) between transmitted code words (CWs), the power allocation mechanism is cascaded to the constellation mapping process of a STBC-CSM scheme, and the optimal power and phase weights for the conveyed information symbols, together with the phases for each CW, are searched by a heuristic algorithm based on differential evolution that yields the best CGD available for the employed CWs. The outcomes of the optimization study, which is focused on maximizing the minimum CGD between all possible CW combinations for different numbers of antennas and modulation schemes, are then used to investigate and exhibit the average enhancements in the communications reliability.

Key words: Space-time block codes, spatial modulation, phase and power allocation

1. Introduction

New wireless communications standards have increasingly required downlink and uplink transmission rates and enhanced spectral efficiencies [1]. Multiantenna transmission and/or reception techniques have been shown to provide significant improvements in either spectral efficiency (i.e. spatial multiplexing) [2] or communications reliability (i.e. enhanced coding gain and diversity orders) [3]. Early designs of spatial multiplexing techniques such as the vertical Bell lab-layered space-time coding (V-BLAST) [2] had a strict constraint about the number of receiving antennas required to achieve considerable error performances; additionally, it suffered from the receiver's decoding complexity. Further research studies proposed the spatial modulation (SM) scheme and introduced its simple transmitter and receiver structures that would cause no additional burden to state-of-the-art encoding and decoding techniques [4]. By conveying extra information via the index of the transmit antenna employed among a multiantenna transceiver end, the SM scheme has provided enhanced spectral efficiencies with the usage of the existing maximum-likelihood (ML)-based or other low-complexity decoding routines [4,5]. The disability of the sole SM scheme at the point of providing transmit diversity was later resolved by combined schemes such as space-time block coded (STBC)-SM [6] that aim to boost the spectral efficiency of the transmission while maintaining a restricted part of the transmit diversity available. The literature consists of several works that have focused on the dual-diversity orthogonal space-time block coding scheme (i.e. Alamouti

*Correspondence: ahmet.coskun@tubitak.gov.tr

STBC [3]), whose spectral efficiency is enhanced by information conveyed by the orthogonal space-time block coded (OSTBC) code word (CW) index. However, it is clear that STBC-SM sacrifices a considerable portion of the available spectral efficiency that would be achieved by a sole SM scheme. Further research has intended to introduce different designs of the combined STBC-SM scheme that would be superior in terms of spectral efficiency and/or communications reliability [7–9]. By introducing the concept of spatial constellation matrices, a high-rate STBC-SM (H-STBC-SM) scheme designed for 4 and 6 transmit antennas was introduced in [7]. Owing to its extended CW set (twice the number of CWs of STBC-SM for the same number of transmit antennas), the H-STBC-SM provided an increase in overall spectral efficiency. Nevertheless, it suffered from degraded error performance when compared to STBC-SM. Another high-rated combination of the STBC and SM schemes, the Complex Interleaved Orthogonal Design SM with the High Degree of Spatial Modulation (CIOD-SM-H), was shown in [8] to provide the same spectral efficiency as the H-STBC-SM, but it exhibited no better error performance than the STBC-SM. The authors of [9] proposed a high-rate spatial modulation scheme by modifying the transmitted CWs due to a cyclic structure (i.e. STBC-CSM). The proposed STBC-CSM scheme was shown to increase spectral efficiency with the help of the extended code set when compared to the pioneering design in [6], resulting in higher spectral efficiencies even when employing fewer transmit antennas. Moreover, the STBC-CSM scheme has achieved considerable coding gain distances (CGDs) between the available CWs that pave the way for operating at lower bit error rates (BERs) when compared to the H-STBC-SM and CIOD-SM-H schemes and at nearly the same BERs as the STBC-SM.

This paper proposes a modified transmitter design based on the high-rate scheme (STBC-CSM) introduced in [9]. With the help of the extensive examination presented in this paper, the modified STBC-CSM design, combined with intersymbol power allocation (ISPA), is shown to achieve lower BERs in Rayleigh-fading environments as a result of the enhanced CGDs between available CWs.

The remainder of this paper is organized as follows. In Section 2, the proposed STBC-CSM scheme employing ISPA at the transmitter is introduced. Section 3 exhibits the optimization process of the proposed scheme in terms of phase and power allocation coefficients related to the CWs and information symbols. Simulation results on the average BER performance of the STBC-CSM with ISPA are provided in Section 4 in order to demonstrate the enhancement in communications reliability. Finally, Section 5 concludes the paper by highlighting the main results.

2. Enhanced STBC-CSM with ISPA

The proposed scheme (STBC-CSM with ISPA) is derived from the high-rate STBC-CSM scheme introduced in [9] with the help of a simple and efficient modification on the signal constellations of the information symbols that are inserted into the transmitted CWs. The STBC-CSM scheme promised to stretch the Euclidean distance between the information-bearing x_1 and x_2 (i.e. increased CGDs between CWs) by employing two different signal constellations, the second of which is rotated by an angle ϕ with respect to the first. With the help of this design, the minimum CGDs were evaluated and exhibited in [9] for different modulation types and a number of transmit antennas. The study in this paper also relies on the basic CW generation mechanism with cyclic structure introduced in [9]. Additionally, by applying power allocation to symbols x_1 and x_2, together with the phase offsetting between them (which is called intersymbol power allocation in this paper), the STBC-CSM scheme with ISPA and its enhancements on the additional coding gains between available CWs and, eventually on the average BER performances, is introduced.

Although the main reference [9] introduced the construction of the STBC-CSM code set (that is also

directly employed within the STBC-CSM with ISPA) in an explicit and detailed manner in order to provide a self-contained study, the basics of the CW construction process are recalled in the following part of this section. A schematic representation of the STBC-CSM and proposed STBC-CSM-ISPA schemes is provided in Figure 1. Here the blocks that are colored in black are common for both schemes; however, the blue and red parts are specific to and only employed by the STBC-CSM and STBC-CSM-ISPA schemes, respectively. In the case of the multiantenna transmitter scheme with n_T antennas, the STBC-CSM code set χ consists of $N_{CB} = n_T - 1$ codebooks (CBs) (i.e. $\chi = \bigcup_{k=1}^{n_T-1} \chi_k$), each including $N_{CW/CB} = n_T$ CWs as defined in [9] as

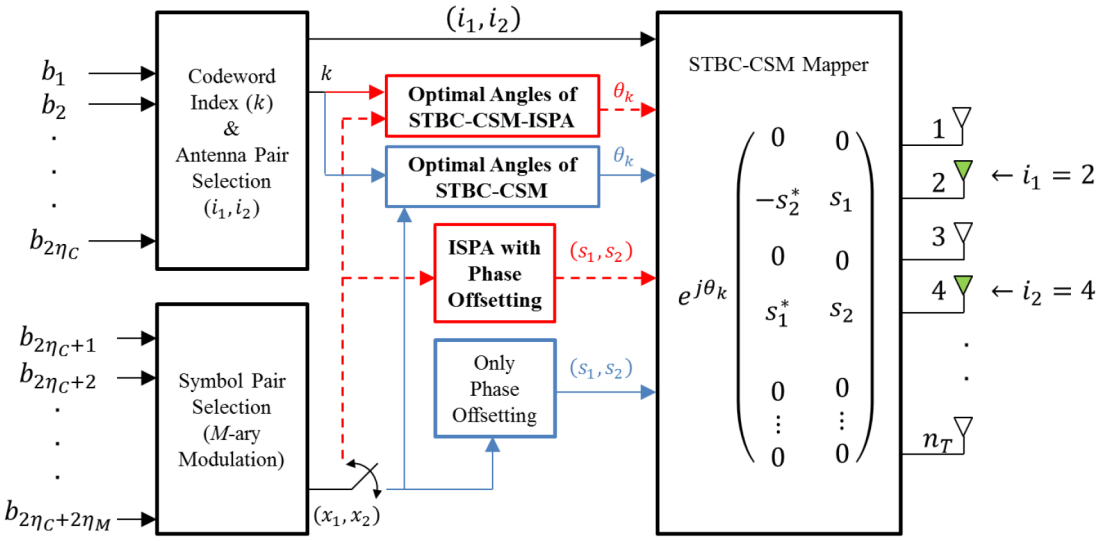

Figure 1. Block diagram representation of the STBC-CSM and STBC-CSM-ISPA schemes.

$$\chi_k = \left\{ \mathbf{G}^{l-1} \mathbf{D}_k e^{j\theta_k} \right\}_{l=1}^{n_T} = \{ \mathbf{X}_{k,l} \}_{l=1}^{n_T}, \; 1 \leq k \leq n_T - 1, \tag{1}$$

where k and l denote the CB and CW indices, respectively. In Eq. (1), $\mathbf{G}^u$ is the u-times right-shifted version of the identity matrix of dimensions $n_T \times n_T$ (i.e. $\mathbf{G}^0 = \mathbf{I}_{n_T}$)

$$\mathbf{G}^u = \begin{bmatrix} 0 & 0 & 1 & 0 \\ 0 & 0 & 0 & 1 \\ 1 & 0 & 0 & 0 \\ 0 & 1 & 0 & 0 \end{bmatrix}_{4\times 4}, \; n_T = 4, \; u = 2, \tag{2}$$

$\mathbf{D}_k$ is the $n_T \times 2$ matrix holding two information symbols x_1 and x_2 consistent with the Alamouti STBC [3]:

$$\mathbf{D}_k = \begin{bmatrix} x_1 & 0 & x_2 & 0 \\ -x_2^* & 0 & x_1^* & 0 \end{bmatrix}^T, \; n_T = 4, \; k = 2, \tag{3}$$
$$\uparrow$$
$$(k+1)^{th}$$

$(\cdot)^T$ is the transpose operator, θ_k is the optimal[1] phase angle of the k^{th} CB, and $\mathbf{X}_{k,l}$ is the l^{th} CW included in the k^{th} CB. By the virtue of its cyclic structure that appears in the code set construction (i.e. in the matrices

[1]The term "optimal" is used to refer to the angle values θ_k, $1 \leq k \leq n_T - 1$ that are obtained by an optimization process that will be introduced in the next section.

$\mathbf{G}$ and $\mathbf{D}$), the STBC-CSM scheme achieves increased spectral efficiencies for any number of transmit antennas, as shown in Table 1 of [9]. Since there are total $N_{CW} = N_{CB}N_{CW/CB} = n_T(n_T - 1)$ CWs, a subset of them with $L_{CW} = 2^{2\eta_C} < N_{CW}$ elements is selected for STBC transmission. Here, $\eta_C = \frac{1}{2}log_2\left(\lfloor N_{CW}\rfloor_{2^p}\right)$ is the spectral efficiency in bits/s/Hertz provided only by the CW index transmission, and $\lfloor\cdot\rfloor_{2^p}$ denotes the nearest power of 2 less than or equal to the argument. Section 4 of [9] provided the best CW subsets that maximize the minimum CGDs (CGD_{min}) for $n_T \in \{3, 4, 5, 6\}$, as given in Table 1. Since the optimality of these CW subsets is validated by [9], they are also employed within the transmission process of the STBC-CSM with ISPA. Differing from the STBC-CSM scheme that inserts two information-bearing digital-modulated symbols x_1 and x_2 into the selected CW, where x_1 is drawn from an M-ary (e.g., M-PSK/M-QAM), constellation Ω_1 and x_2 are drawn from the rotated version of the M-ary constellation Ω_1 (i.e. $\Omega_2 = \Omega_1 e^{j\phi}$). Differing from STBC-CSM, the STBC-CSM with ISPA employs two symbols that are drawn from scaled versions of Ω_1 and Ω_2 (i.e. $\Omega_1^{'} = \sqrt{p}\,\Omega_1$ and $\Omega_2^{'} = \sqrt{1-p}\,\Omega_2 = \sqrt{1-p}\,\Omega_1 e^{j\phi}$) by maintaining the total squared mean of the symbols as unity. This simple modification in the employed signal constellations paves the way for the enhancement of the minimum CGDs between transmitted CWs, resulting in lower BERs when compared to the original STBC-CSM scheme. However, the overall spectral efficiency of the proposed STBC-CSM with ISPA is the same as that of STBC-CSM:

Table 1. Optimal CWs that maximize the minimum CGDs for $n_T \in \{3, 4, 5, 6\}$.

n_T	Optimal CWs
3	$\mathbf{X}_{1,1},\ \mathbf{X}_{1,2},\ \mathbf{X}_{2,1},\ \mathbf{X}_{2,2}$
4	$\mathbf{X}_{1,1},\ \mathbf{X}_{1,2},\ \mathbf{X}_{1,3},\ \mathbf{X}_{1,4},\ \mathbf{X}_{2,1},\ \mathbf{X}_{2,2},\ \mathbf{X}_{3,1},\ \mathbf{X}_{3,3}$
5	$\mathbf{X}_{1,1},\ \mathbf{X}_{1,2},\ \mathbf{X}_{1,3},\ \mathbf{X}_{1,4},\ \mathbf{X}_{2,1},\ \mathbf{X}_{2,2},\ \mathbf{X}_{2,3},\ \mathbf{X}_{2,4},\ \mathbf{X}_{3,1},\ \mathbf{X}_{3,2},\ \mathbf{X}_{3,3},\ \mathbf{X}_{3,4},\ \mathbf{X}_{4,1},\ \mathbf{X}_{4,2},\ \mathbf{X}_{4,3},\ \mathbf{X}_{4,4}$
6	$\mathbf{X}_{1,1},\ \mathbf{X}_{1,3},\ \mathbf{X}_{1,5},\ \mathbf{X}_{1,6},\ \mathbf{X}_{2,1},\ \mathbf{X}_{2,4},\ \mathbf{X}_{2,6},\ \mathbf{X}_{3,1},\ \mathbf{X}_{3,2},\ \mathbf{X}_{3,3},\ \mathbf{X}_{4,1},\ \mathbf{X}_{4,4},\ \mathbf{X}_{4,5},\ \mathbf{X}_{5,1},\ \mathbf{X}_{5,3},\ \mathbf{X}_{5,5}$

$$\eta_T = \eta_C + \eta_M = \frac{1}{2}log_2\left(\lfloor N_{CW}\rfloor_{2^p}\right) + log_2\left(M\right) \tag{4}$$

As outlined in Figure 1, depending on the input information-bearing bits $\mathbf{b_l l = 12}, \ldots, \mathbf{2}\eta_\mathbf{T}$, the antenna indices (i.e. $\mathbf{i_1}$ and $\mathbf{i_2}$) (hence the CW index $\mathbf{k}$) and the modulated symbols (i.e. $\mathbf{s_1}$ and $\mathbf{s_2}$) are determined. The Alamouti CW, distributed over two consecutive transmission intervals and $\mathbf{n_T}$ spatial channels (only two of which are activated), is transmitted over the quasistatic Rayleigh-fading channels $\mathbf{H}$ and received through $\mathbf{n_R}$ antennas. If the CW $\mathbf{X_{k,l}}$ is constructed at the transmitter due to the input bit stream, the received signal matrix of dimensions $\mathbf{n_R}\times\mathbf{2}$ is expressed as follows [6]:

$$\mathbf{y} = \sqrt{\frac{E_s}{2N_o}}\mathbf{H}\mathbf{X}_{k,l} + \mathbf{N} \tag{5}$$

where E_s and N_o denote the average symbol energy for each CW and the one-sided power spectral density of the additive white Gaussian noise at each receive antenna, respectively. In addition, $\mathbf{H}$ and $\mathbf{N}$ are the channel and noise matrices with dimensions $n_R \times n_T$ and $n_R \times 2$ whose entries are assumed to be independent and identically distributed (i.i.d.) complex Gaussian random variables, each with zero mean and unit variance. The channel matrix is assumed to remain constant during the transmission of each CW and to independently vary from one CW to another.

We assume that channel matrix $\mathbf{H}$ is perfectly known at the receiver. The receiver sides of the STBC-CSM and STBC-CSM-ISPA schemes both employ the ML decoding mechanism defined by Eqs. (15)–(19) in [6]. Hence, it can clearly be seen that the modification proposed in this paper would cause no additional complexity in the aforementioned ML decoder for the STBC-SM. The ML-based decoding mechanism, whose complexity has the tendency to linearly increase with respect to $\mathbf{L_{CW}}$ and $\mathbf{M}$, can be easily employed within the STBC-CSM scheme with ISPA. Note that the inclusion of power allocation with phase offsetting might cause impairments in the transmit power management of wireless communications setups that employ PSK or similar modulation types with constellation points of constant magnitude due to possible limitations at the power amplifier outputs. However, this would probably cause no additional consideration or limitation in the transmitter ends of forthcoming and next-generation wireless communications systems as they are expected to be much more immune to this type of problem and employ nonconstant amplitude, high-level signal constellations such as 16-QAM and 64-QAM.

3. Optimization of the proposed scheme

This section aims to explore the optimal values of the power allocation coefficient p, the constellation rotation angle ϕ, and the phase angles of CBs θ_k, $1 \leq k \leq n_T - 1$ that achieve the maximum value of CGD for the employed CWs and modulation symbols. In order to provide a search in the multidimensional parameter space constituted by ϕ and θ_k, $1 \leq k \leq n_T - 1$, the objective function to be maximized is selected as the minimum CGD of constructed code set χ for given n_T and the modulation type:

$$CGD_{min}\left(\chi; p,\, \phi, \theta_1, \theta_2, \ldots, \theta_{n_T-1}\right) = \min_{n,m,n\neq m}\left\{\min_{r,t}\left\{\min_{s_1,s_2,\hat{s}_1,\hat{s}_2}\left\{\det\left\{\Theta_{n,m,r,t}\left(s_1,s_2,\hat{s}_1,\hat{s}_2\right)\right\}\right\}\right\}\right\} \tag{6}$$

In Eq. (6), $det?(\cdot)$ denotes the matrix determinant operator, and the pairs $s_1\hat{s}_1$ and $s_2\hat{s}_2$ are modulated symbols drawn from the signal constellations $\Omega_1^{'}$ and $\Omega_2^{'}$, respectively, and

$$\Theta_{n,m,r,t}\left(s_1,s_2,\hat{s}_1,\hat{s}_2\right) \triangleq \left(\mathbf{X}_{n,r}\left(s_1,s_2\right) - \mathbf{X}_{m,s}\left(\hat{s}_1,\hat{s}_2\right)\right)^H \times \left(\mathbf{X}_{n,r}\left(s_1,s_2\right) - \mathbf{X}_{m,s}\left(\hat{s}_1,\hat{s}_2\right)\right) \tag{7}$$

where $(\cdot)^H$ is the Hermitian transpose of matrix argument $\mathbf{X}_{k,l}\left(s_1,s_2\right)$, $1 \leq k,l \leq n_T - 1$, $s_i \in \Omega_i^{'}$, $i = 1,2$, denotes the modulated CW that is constructed via the insertion of M-ary baseband symbols s_1, s_2 into the l^{th} CW included in the k^{th} CB. Hence, the optimal values can be found by maximizing Eq. (6):

$$\left\{p^*,\, \phi^*, \theta_1^*, \theta_2^*, \ldots, \theta_{n_T-1}^*\right\} = \arg\left\{\min_{p,\phi,\theta_1,\theta_2,\ldots,\theta_{n_T-1}}\left\{CGD_{min}\left(\chi; p,\, \phi, \theta_1, \theta_2, \ldots, \theta_{n_T-1}\right)\right\}\right\} \tag{8}$$

For these kinds of optimization purposes, the research in the literature has employed different optimization search algorithms, including the analytical and exhaustive search methods. Although the exhaustive search method might respond in tolerable time intervals for the objective functions modeled via single or two-dimensional parameter spaces, increasing dimensions (e.g., three or more) in the search space occur at unmanageable computer run times, as stated in Section II-A of [6]. Since the objective function given in Eq. (6) for the STBC-CSM with ISPA is $(n_T + 1)$-variate function, the exhaustive (brute force) and analytical search mechanisms would not help to explore the CGD maxima that is achieved by the optimal power and phase coefficients p^*, ϕ^*, θ_k^*, $1 \leq k \leq n_T - 1$. Consequently, within this study, a heuristic algorithm based on the differential evolution (DE) method is preferred because it provides solutions in reasonable and affordable durations. A

detailed explanation about the simple and efficient DE algorithm is given in [10]. The parameters F and CR of the DE algorithm that control the amplification of the differential variation and crossover rate, respectively, are initialized as $F = 1.0$ and $CR = 0.5$. The optimal values maximizing the minimum CGDs are later evaluated for BPSK, QPSK, 8-QAM, and 16-QAM modulations with $n_T \in \{3, 4, 5, 6\}$ and are listed in Table 2, together with the corresponding maximum CGD values. The variation of CGD is compared for both schemes (STBC-CSM and STBC-CSM with ISPA) in Figure 2 and Figure 3 for several modulation schemes and a number of transmit antennas. In Figure 2, the variation of minimum CGDs for four different modulation schemes is depicted with respect to the phase angle of the second CB (i.e. θ_2).

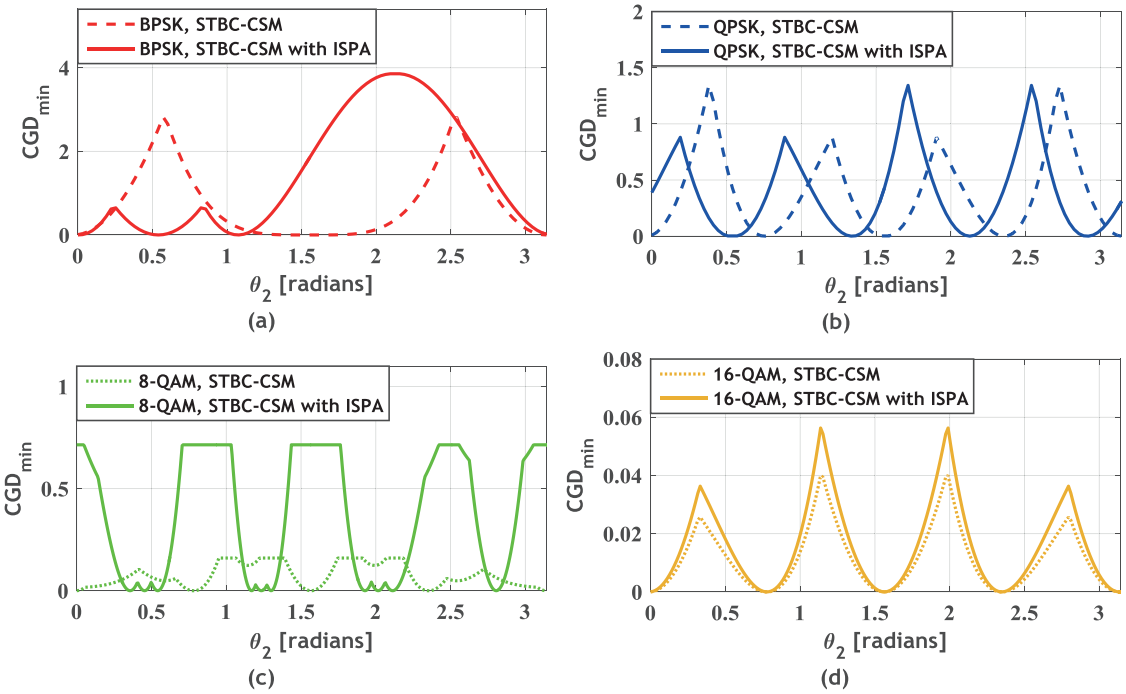

Figure 2. Comparison of the CDG variations of the STBC-CSM and STBC-CSM with ISPA for $n_T = 3$ and a) BPSK; b) QPSK; c) 8-QAM; d) 16-QAM modulations.

In order to be able to demonstrate the dependency of $(n_T + 1)$-variate minimum CGDs, the first $n_T = 3$ parameters (i.e. p, ϕ, and θ_1) are set with the optimal values given in Table 2. As seen from the curves given in Figure 2a for $n_T = 3$, the minimum CGDs that play a critical role in the error performance of STBC-based schemes are increased for BPSK, 8-QAM, and 16-QAM modulations by the inclusion of ISPA within the STBC-CSM scheme. However, in the case of QPSK, the maximum value of the minimum CGDs are the same for both schemes as can be seen by comparing the second row of Table 2 and Table 2 of [9]. Although the maximum values of the CGDs are identical, the variation of minimum CGDs are seen to be different from each other since the optimized objective function has a periodic nature with respect to the angular domain. The subfigures in Figure 3 depict the maximum values of the minimum CGDs that are evaluated for the BPSK, QPSK, 8-QAM, and 16-QAM modulations (i.e. $\eta_M = 1, 2, 3$ and 4) and for $n_T \in \{3, 4, 5, 6\}$. By examining the maximum values of CGDs for both schemes, it can clearly be seen that, except in the case of QPSK with $n_T = 3$, the STBC-CSM with ISPA enhances the CGDs provided by the STBC-CSM scheme for all cases considered. This, in turn, leads to the decreased probability of CWs misdetections (i.e. lower BERs) in communications environments with Rayleigh-fading and Gaussian noise characteristics.

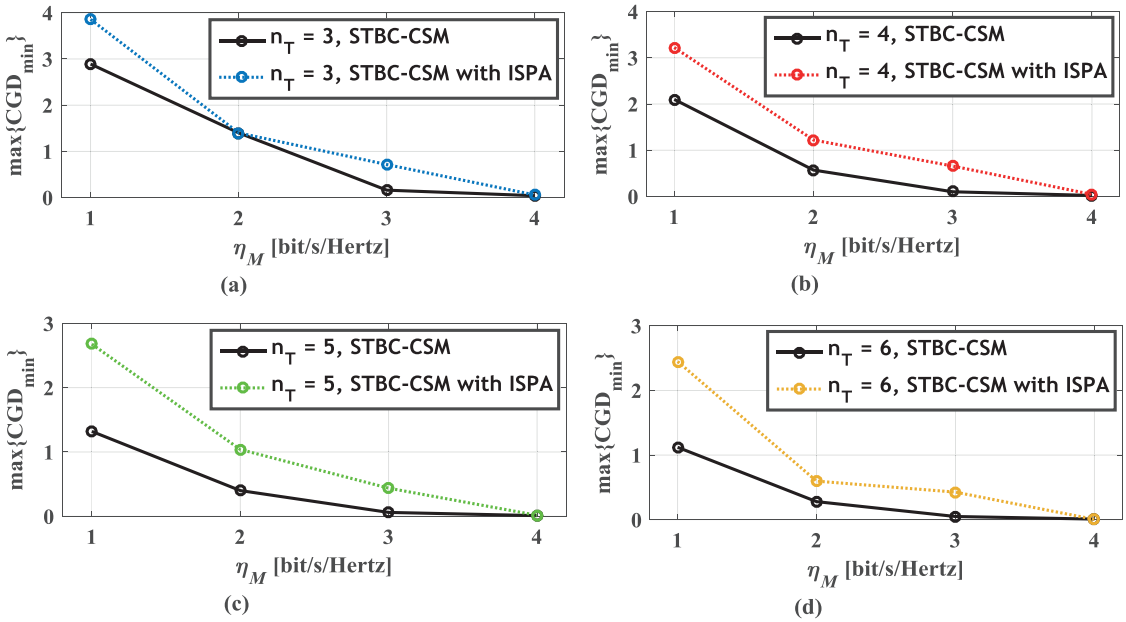

Figure 3. Variation of the minimum CGD values of both schemes due to the spectral efficiency of modulation schemes (i.e. corresponding to BPSK, QPSK, 8-QAM, and 16-QAM constellations) for a) $n_T = 3$; b) $n_T = 4$; c) $n_T = 5$; d) $n_T = 6$.

Table 2. Optimal values of p, ϕ, and θ_k, $1 \leq k \leq n_T - 1$ and corresponding maximum CGD values achieved by the STBC-CSM with ISPA.

n_T	Mod.	p^*	ϕ^*	θ_1^*	θ_2^*	θ_3^*	θ_4^*	θ_5^*	$\{CGD_{min}\}$
3	BPSK	0.75	0.63	0.54	2.11	-	-	-	3.86
	QPSK	0.50	0.79	2.13	1.70	-	-	-	1.40
	8-QAM	0.62	0.88	1.23	1.51	-	-	-	0.71
	16-QAM	0.58	0.79	1.59	2.01	-	-	-	0.06
4	BPSK	0.78	0.52	3.09	0.99	2.04	-	-	3.22
	QPSK	0.72	0.79	1.31	2.31	1.17	-	-	1.21
	8-QAM	0.52	0.73	1.11	3.04	1.67	-	-	0.66
	16-QAM	0.72	0.79	1.15	1.72	2.29	-	-	0.04
5	BPSK	0.80	0.39	1.99	2.77	1.20	0.42	-	2.68
	QPSK	0.74	0.79	2.78	2.34	0.41	1.59	-	1.04
	8-QAM	0.61	0.85	1.24	2.25	1.07	3.07	-	0.44
	16-QAM	0.65	0.86	2.20	1.14	1.39	0.19	-	0.02
6	BPSK	0.80	0.31	1.03	2.91	0.40	1.66	2.28	2.45
	QPSK	0.72	0.68	0.53	1.13	3.05	0.19	2.37	0.60
	8-QAM	0.61	1.02	1.60	0.71	0.93	2.13	2.85	0.43
	16-QAM	0.86	1.25	1.59	0.68	0.37	3.02	1.27	0.01

4. Simulation results on BER performances

This section presents simulation results related to the average BER performances of STBC-CSM with ISPA and STBC-CSM schemes in Rayleigh-fading channels. The average BER performances of the STBC-SM and V-BLAST schemes are provided in Figures 4–8 as benchmarks. For the same spectral efficiency η_T, the STBC-CSM scheme is shown in [9] to achieve the same average BER levels of the STBC-SM [6], despite the use of

fewer transmit antennas and is shown to be superior to other existing schemes such as the H-STBC-SM [7] and CIOD-SM-H [8]. Hence, the simulation results of the STBC-CSM with ISPA are compared with the results of the STBC-CSM, STBC-SM [6], and V-BLAST schemes [2], employing a minimum mean square error detector with ordered successive interference cancellation (MMSE-OSIC). In order to exhibit the enhancements achieved by the inclusion of ISPA within the STBC-CSM scheme, numerous Monte Carlo simulations are performed for miscellaneous transmission and reception scenarios and demonstrated in Figures 4–8. By considering that the average symbol energy per transmitted CW is unity ($E_s = 1$), the variation of the average BER performances is examined for maximal-ratio combining receiver ends. Figure 4 shows the average error rate variation of 16-QAM signals for the STBC-CSM and STBC-CSM-ISPA schemes with $n_T = 3$ and $n_R \in \{1, 2, 3\}$. For the same spectral efficiency of $\eta_T = 5$ bits/s/Hertz, STBC-SM scheme $\{n_T = 4$, 16-QAM, $n_R \in \{1, 2, 3\}$, $\eta_T = 5$ bits/s/Hertz$\}$ and for the spectral efficiencies of $\eta_T = 4$ bits/s/Hertz and 6 bits/s/Hertz, V-BLAST scheme $\{n_R = 3$, QPSK, $n_T \in \{2, 3\}\}$ are considered in order to be compared in terms of average BER performance. As seen from the curves in Figure 4, the STBC-SM scheme $\{n_T = 4$, 16-QAM, $n_R \in \{1, 2, 3\}$, $\eta_T = 5$ bits/s/Hertz$\}$ and V-BLAST scheme $\{n_T = 2$, QPSK, $n_R = 3$, $\eta_T = 4$ bits/s/Hertz$\}$ are superior to the considered STBC-CSM and STBC-CSM-ISPA schemes; however, the former employs more transmit antennas and the latter achieves a lower spectral efficiency. Furthermore, the inclusion of the ISPA mechanism within the STBC-CSM scheme is seen to provide additional average SNR gains of 0.13 dB, 0.27 dB, and 0.32 dB for $n_R \in \{1, 2, 3\}$, respectively.

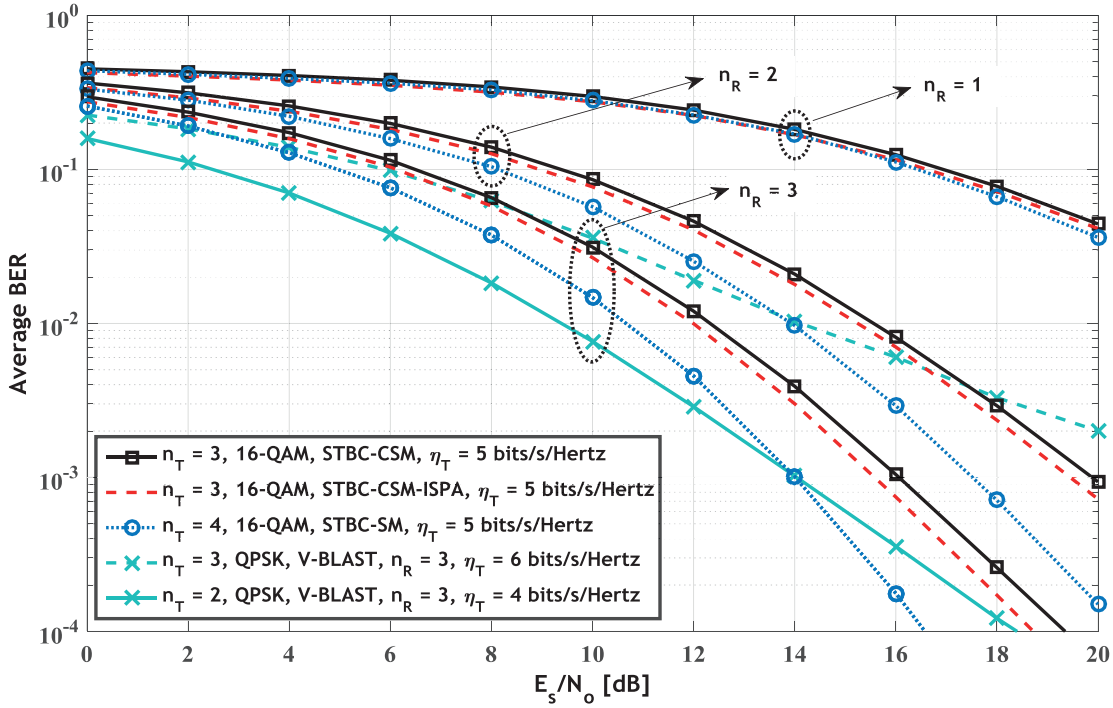

Figure 4. BER comparison of the STBC-CSM-ISPA $n_T = 3$, 16-QAM, $n_R \in 1, 2, 3$, $\eta_T = 5$ bits/s/Hertz to other SM schemes with $\eta_T \in 4, 5, 6$ bits/s/Hertz.

Similarly, Figures 5–8 depict the average BER performances and provide a comparison of the STBC-CSM and STBC-CSM-ISPA schemes for $n_T = 4$ with QPSK signals, $n_T = 5$ with 8-QAM signals, $n_T = 6$ with BPSK signals, and $n_T = 5$ with 16-QAM signals, respectively. Figures 5–8 also include the average BER performances

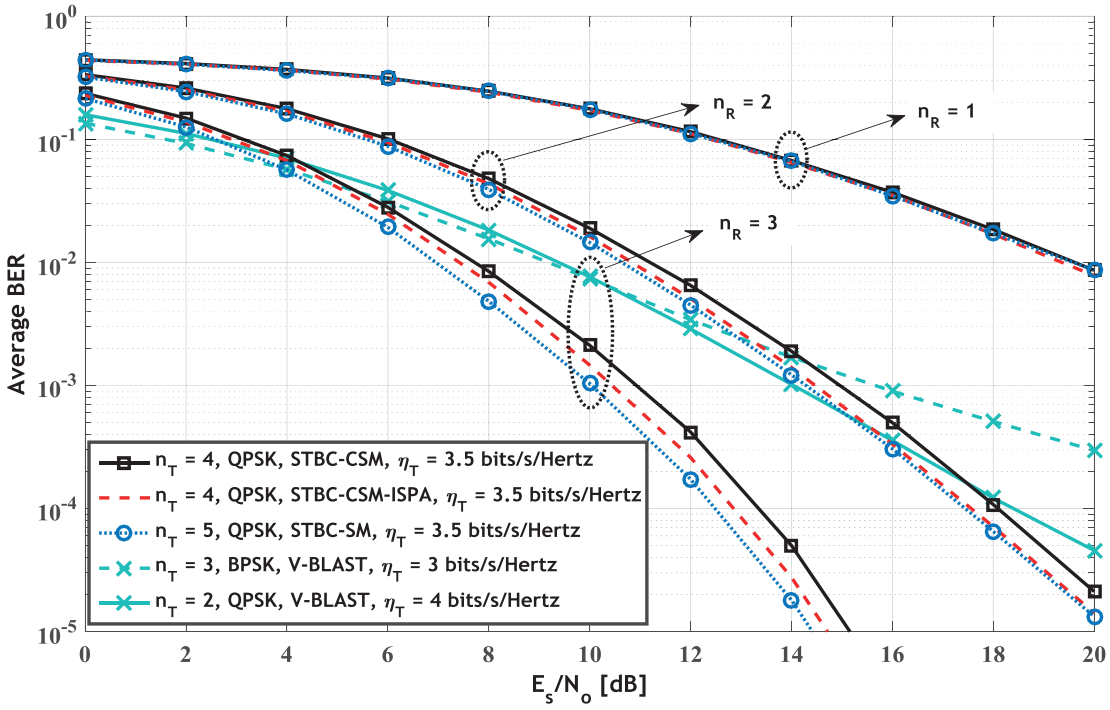

Figure 5. BER comparison of the STBC-CSM-ISPA $n_T = 4$, QPSK, $n_R \in 1, 2, 3$, $\eta_T = 3.5$ bits/s/Hertz with other SM schemes of $\eta_T \in 3, 3.5, 4$ bits/s/Hertz.

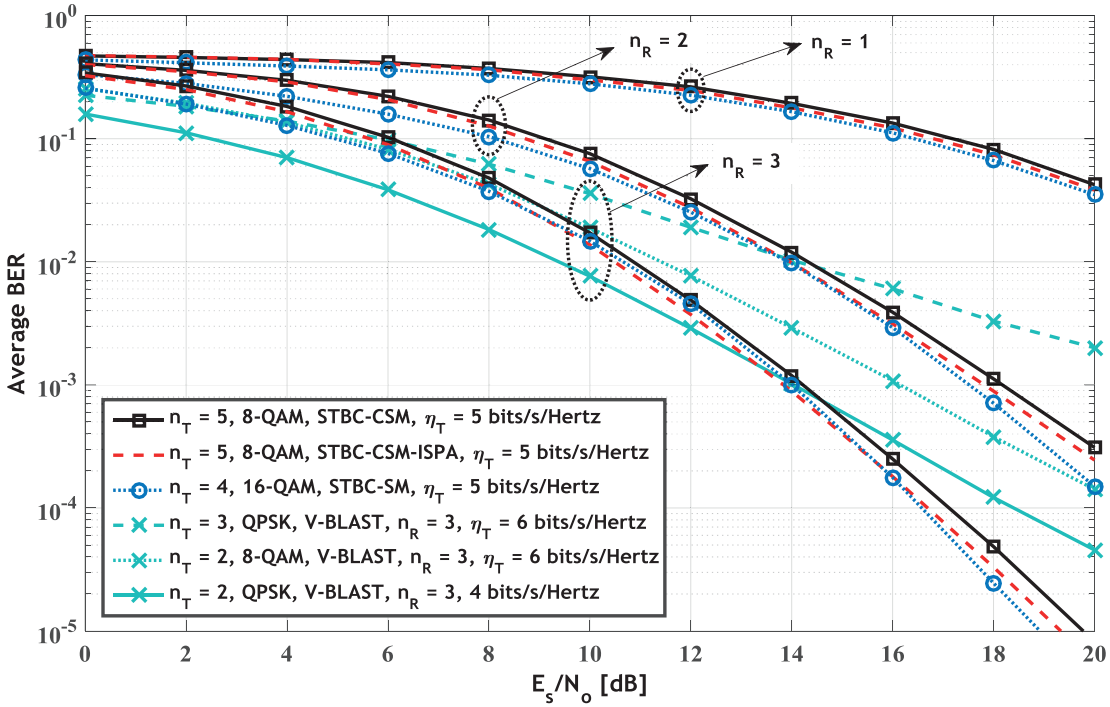

Figure 6. BER comparison of the STBC-CSM-ISPA $n_T = 5$, 8-QAM, $n_R \in 1, 2, 3$, $\eta_T = 5$ bits/s/Hertz to other SM schemes with $\eta_T \in 4, 5, 6$ bits/s/Hertz.

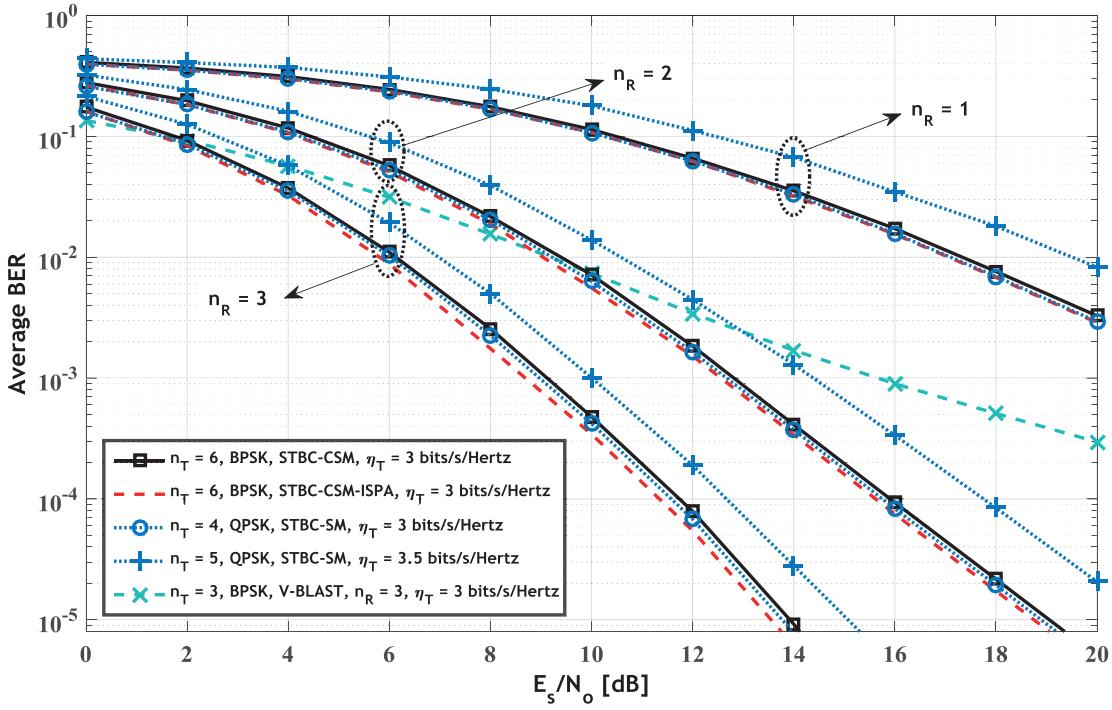

Figure 7. BER comparison of the STBC-CSM-ISPA $n_T = 6$, BPSK, $n_R \in 1, 2, 3$, $\eta_T = 3$ bits/s/Hertz to other SM schemes with $\eta_T \in 3, 3.5$ bits/s/Hertz.

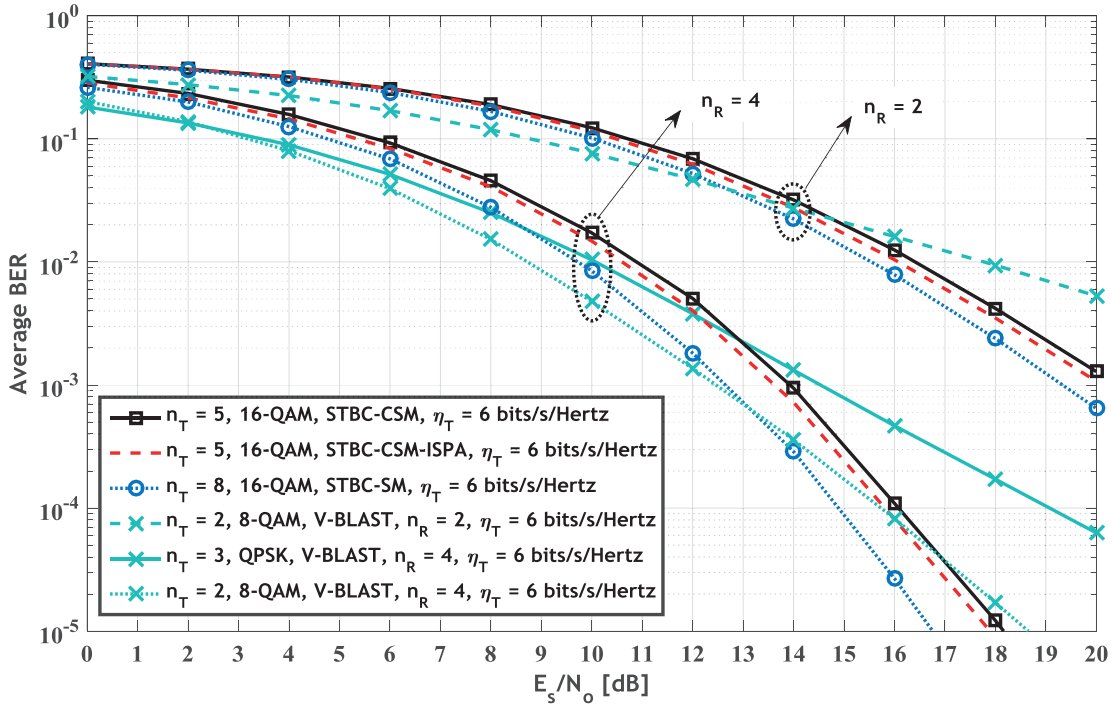

Figure 8. BER comparison of the STBC-CSM-ISPA $\{n_T = 5$, 16-QAM, $n_R \in \{2, 4\}$, $\eta_T = 6$ bits/s/Hertz$\}$ to other SM schemes with $\eta_T = 6$ bits/s/Hertz.

of STBC-SM and V-BLAST configurations that achieve the same and/or close spectral efficiencies in order to extend the perspective of the performance comparison. As seen in all of the figures, the STBC-CSM scheme with ISPA achieves lower average BER levels when compared to the STBC-CSM scheme. From the perspective of transmit power consumption, the advantage provided in BER levels for the investigated scenarios would simply pave the way for STBC-CSM schemes with ISPA to operate at the same BER levels as STBC-CSM schemes with reduced transmit power or signal-to-noise ratio (SNR) requirements. The average SNR gains provided by the inclusion of ISPA within the STBC-CSM scheme are extracted from each figure and tabulated in Table 3. The average SNR gains given in Table 3 clearly indicate the potential advantages (and reductions in average BER levels) provided by the STBC-CSM with ISPA. By examining the content of Table 3, one can easily realize that the average SNR gains have the tendency to increase with the increasing value of the receiver antennas. Here it can be noted that BER curves given in Figures 6 and 8 that depict the performance of the STBC-CSM scheme with two receiver antennas ($n_R = 2$) for cases $n_T = 5$, 8-QAM and $n_T = 5$, 16-QAM are consistent with those plotted in Figure 3 of [9]. Moreover, the average BER performance of the STBC-SM $\{n_T = 8$, 16-QAM, $n_R = 4$, $\eta_T = 6$ bits/s/Hertz$\}$ configuration is depicted in Figure 8 and is in perfect agreement with the one provided in Figure 8 of [6].

Table 3. Average SNR gains in dB observed in a high-SNR region of Figures 48.

	Average SNR gains in dB for all scenarios				
n_R	$n_T = 3$, 16-QAM	$n_T = 4$, QPSK	$n_T = 5$, 8-QAM	$n_T = 6$, BPSK	$n_T = 5$, 16-QAM
1	0.13	0.14	0.30	0.22	-
2	0.27	0.36	0.35	0.29	0.33
3	0.32	0.45	0.45	0.35	-
4	-	-	-	-	0.40

5. Conclusion

The examination presented in this paper has provided a brief and insightful look at the advantages achieved by including the combined ISPA mechanism within the STBC-CSM scheme. The optimal power allocation coefficients and phase angles that are shown to yield more coding gains are searched by a heuristic DE algorithm. With the help of the optimal values evaluated through the optimization process, the proposed scheme (STBC-CSM with ISPA) is shown to achieve increased minimum CGDs that directly result in enhanced BER performances (more specifically, average SNR gains of up to 0.45 dB with respect to the reference STBC-CSM design of [9]). Consequently, the proposed inclusion strengthens the communications reliability of the reference design STBC-CSM, whose spectral efficiency has already been shown to be assertive when compared to other existing SM-based and related schemes such as STBC-SM, H-STBC-SM, CIOD-SM-H, and V-BLAST-MMSE-OSIC.

References

[1] Molisch AF. Wireless Communications. 2nd ed. New York, NY, USA: IEEE Press/Wiley, 2011.

[2] Wolniansky PW, Foschini GJ, Golden GD, Valenzuela RA. V-BLAST: an architecture for realizing very high data rates over the rich-scattering wireless channel. In: International Symposium on Signals, Systems, and Electronics; 29 September–2 October 1998; Pisa, Italy. New York, NY, USA: IEEE. pp. 295-300.

[3] Alamouti SM. A simple transmit diversity technique for wireless communications. IEEE J Sel Area Comm 1998; 16: 1451-1458.

[4] Mesleh R, Haas H, Ahn CW, Yun S. Spatial modulation–a new low complexity spectral efficiency enhancing technique. In: Conference on Communications and Networking in China; 25–27 October 2006; Beijing, China. New York, NY, USA: IEEE. pp. 1-5.

[5] Jeganathan J, Ghrayeb A, Szczecinski L. Spatial modulation: optimal detection and performance analysis. IEEE Commun Lett 2008; 12: 545-547.

[6] Başar E, Aygölü Ü, Panayırcı E, Poor HV. Space-time block coded spatial modulation. IEEE T Commun 2011; 59: 823–832.

[7] Le MT, Ngo VD, Mai HA, Tran XN. High-rate space-time block coded spatial modulation. In: IEEE Advanced Technologies for Communications 2012; 10–12 October 2012; Hanoi, Vietnam. New York, NY, USA: IEEE. pp. 278-282.

[8] Rajashekar R, Hari KVS. Modulation diversity for spatial modulation using complex interleaved orthogonal design. In: IEEE Region 10 Conference 2012; 19–22 November 2012; Quezon City, Philippines. New York, NY, USA: IEEE. pp. 1-6.

[9] Li X, Wang L. High rate space-time block coded spatial modulation with cyclic structure. IEEE Commun Lett 2014; 18: 532-535.

[10] Storn R, Price K. Differential evolution-a simple and efficient heuristic for global optimization over continuous spaces. J Global Optim 1997; 11: 341-359.